CNRS
Centre National de la Recherche Scientifique

INFN
Instituto Nazionale di Fisica Nucleare

The ESQB mechanical resonances analysis

M. Eisenmann

VIR-0665A-20

July 10, 2020

VIRGO * A joint CNRS-INFN Project
Project office: Traversa H di via Macerata - I-56021 S. Stefano a Macerata, Cascina (PI)
Secretariat: Telephone (39) 50 752 521 – Fax (39) 50 752 550 – e-mail virgo@pisa.infn.it

Contents

1 Introduction

Frequency-independent squeezed states have been injected into the Virgo detector during the O3 run. This allowed to improve the Virgo sensitivity sprectum over few hundreds Hertz and therefore its BNS range.

Several components had to be installed in the Virgo detection lab in order to reduce the optical losses and phase-noise seen by the squeezed vacuum state.

These components have been installed on the External Squeezer Bench (ESQB) represented figure 1

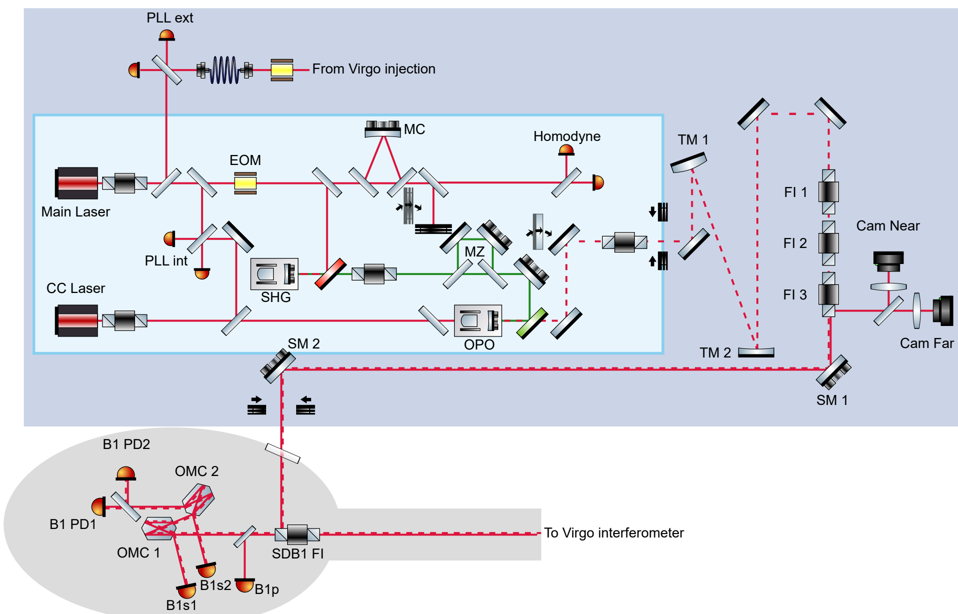

Figure 1: Simplified optical scheme of the ESQB components.

As can be seen on this figure, several components are required

During the squeezing commissioning activities, the frequency-independent squeezed vacuum states have been injected into the Virgo detector. Figure 2 shows one of the first injection of the squeezed beam. It compares the Virgo sensitivities with and without the squeezing injection.

Because the alignment and controls were not optimized at that point, optical losses and phase-noise degraded too much the squeezing quality to see any improvement of the Virgo sensitivity at high-frequency.

However, a broadband degradation at low-frequency as well as few peaks are visibles in the sensitivity. These two effects are symptomatic of scattered light recombining with the Virgo main laser beam and being detected at the B1 photodiodes. This figure particulary highlight the threat of scattered light for interferometric gravitational waves detectors as it affects their sensitivity below few hundreds Hertzs where most of the BNS and BBH signals are expected.

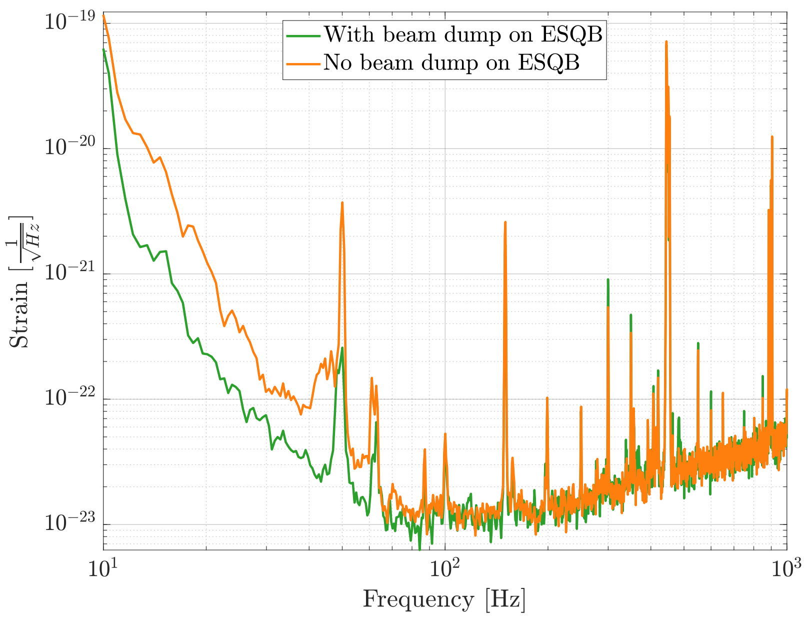

Figure 2: Virgo sensitivity around the first squeezing injection with and without a beam dump on the ESQB with a poor squeezer alignment and controls not optimized.

Few mechanisms could be responsible for such light.

- First, the OPO reflectivity, residual reflections on anti-reflective coatings can be sources of back-reflected light into the interferometer. It has been computed that the OPO is the main source of back-scattered light inside the squeezer box [1]. However, the installation of three Faraday isolators with total isolation factor of 120 dB (or 40dB each) between the squeezer box and the Virgo interferometer was enough to reduce this effect more than a factor ten below Virgo sensitivity. This factor ten being the standard tolerated level of technical noises at Virgo.
- Dust particles located on optical components and hit by the beam will be source of scattered light. Therefore the squeezer components were installed inside a box.

  However, optical components required for the squeezed light injection were also susceptibles to be affected by dusts particles. And it has been found out during commissioning activities that a lot of dust was present both on optical components as well as on the SDB1 Viewport pipe. After careful cleaning of these components, a plexiglas enclosure has been installed above the ESQB to prevent dust particles. In addition, an airflow was used during each commissioning activities requiring to open this plexiglas enclosure so that dust particles would be pushed outside this enclosure.

The careful cleaning and plexiglas enclosure should mitigate back-scattered light due to this effect.

- Another possible source of back-scattered light into the interferometer is a misaligned beam hitting optical mounts. Again, because of the three Faraday isolators installed on the ESQB, it can be expected that only components between the FI3 and the SDB1 might induce such spurious light. This include both Cam Far and Cam Near, crystal and polarizer of FI3, SM1 and SM2 and the SDB1 Viewport.

  If a beam hits one of these components mounts, any mechanical resonance of this component mount can imprint an excess of noise at the component mechanical resonance frequency. To limit this effect, ESQB has been installed inside an acoustic enclosure which should isolate the ESQB and the components installed on it from the acoustic noise. Furthermore, the ESQB optical bench is installed on a rigid steel frame mounted on elastomer pads so to limit the seismic motions that could excit mechanical resonances.

The last item from this list, namely scattered light due to optical component mechanical resonance, was particulary troublesome. The next sections will present the activities performed to mitigate its effect on the Virgo sensitivity.

2 Shaking and tapping tests measurement

Figure 2 highlighted some possibles effects that can be induced by scattered light from the squeezer optics. The peaks present on this figure are due to a spurious beam hitting an optical component which mechanical resonance couples to an optical path difference. Therefore, this effect can be mitigated by finding the mechanical resonance frequency of optical components on the squeezed beam path.

Because in normal condiditions the seismic ground activities are too low to excite all the ESQB mechanical resonances, shaking and tapping of the ESQB optical bench and components have been performed. This allows indeed to excite these mechanical resonances and ease their detections.

The ESQB optical breadboard was shaken by hand in its short and long directions. Three ultra low frequency seismic accelerometers Wilcoxon Research model 731-207 have been installed on ESQB which sense acceleration noise in every degree of freedom. They are labelled in the following '*X axis*' which senses acceleration noise in the short direction of ESQB (ie parallel to the Faraday isolators chain), '*Y axis*' for the vertical direction and '*Z axis*' for the long direction of ESQB.

Because of the three Faraday isolators chain, the scattered light induced before them is greatly reduced. Therefore, only the components between the SDB1 and the FI3 components have been tested. This includes the SDB1 viewport, the SM1 and SM2, the Cam Near and Cam Far, and the FI3 polarizer, polarizer base and magnet.

The ESQB optical components mechanical resonances have been excited using the ICP Impulse Force Test Hammer model 086C01. This hammer provides a broadband nearly-constant force and was used in every degrees of freedom close to the tested optical component.

The ICP mini accelerometer model 352C68 was mounted on each tested component. Because it weights only two grams, it should not affect the weight distribution of the tested component and therefore allows to not distord its mechanical resonance frequency. It will be named '*Mini Acc*' in the following sections.

3 The ESQB mechanical resonances analysis

First, ESQB mechanical resonances have been measured.

Figure 3 shows the resulting acceleration noises sensed by X Y and Z accelerometers from top to bottom plots. On each plot, the blue curve represent the quiet reference spectrum, the orange curve the X excitation spectrum and red curve the Z excitation spectrum between 1 and 1 000 Hz. The FFT used to compute these spectrums has a 0.15Hz precision.

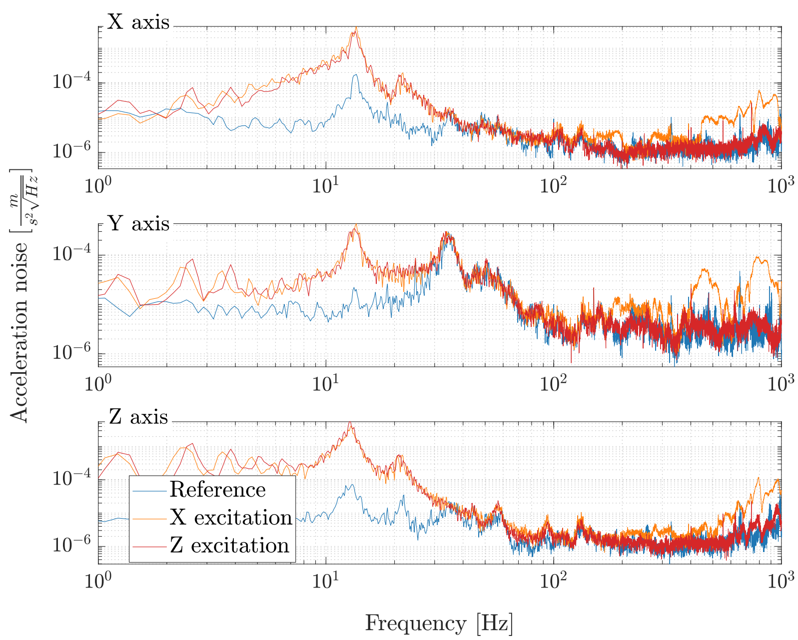

Figure 3: Shaking tests on ESQB.

From this figure, several peaks that are not present in the quiet reference spectrum appear. They correspond to mechanical resonances of ESQB that are excited by the shaking of the bench.

It can also be seen that for some frequencies, peaks are present both in reference spectrum and excited spectrums. This means that the excitation has no impact on the acceleration noise at this particular frequency. This could be due to another source of excitation (eg the airflow which is always turned on during commissioning activities in the detection lab) or another component mechanical resonance.

In order to extract the mechanical resonances of the ESQB, the mean spectrum of all sensor for each excitation has been computed.

First, the peaks due to the 50Hz of the power grid and its harmonics may appear on some spectrums and spoil the analysis. Therefore, for all frequency close to 50Hz and its harmonics (where the 'closeness' is estimated using modulo of the frequency with respect to 50Hz,eg between 49.59 Hz and 50.35Hz for the 50Hz line), the spectrum values have been replaced by constant value. This constant value is taken at the last frequency which has a modulo above 0.41 (eg 49.43Hz for the 50hz case). This frequency window was empirarically chosen so to properly remove all 50 Hz harmonics.

Then, a sliding mean filter has been applied to the reference and excitations spectrums. In order to keep low-frequency information while smoothing the high-frequency data, the number of points used in the mean computation increases as $\frac{f}{11}$ and $\frac{f}{1}$ for respectively the excited and reference spectrums. These frequency windows are empirically chosen and used at each frequency to compute the mean value of the spectra. Furthermore, the reference is more smoothed than the excited spectra in order to remove possible excitations during the measurement and to be sure to only keep the background noise. The smoothing is performed three times so to avoid discontinuity in the smoothed spectrums.

The smoothed reference spectrum defines hereafter the background spectrum. Altough this procedure will distord the peak height, it will not changed the peak location. And can therefore be used to extract each peak frequency. Then, the peak height are the compared with the background level so to extract a Signal-to-Noise Ratio (SNR) of each peak. As the smoothing is distording the peak height, the non-smoothed spectrum levels at each peak frequency are used to estimate this SNR. And only peak with SNR above 9 are kept.

This analysis is presented figure 4. The reference, X and Z excitation spectrums are respectively the gray, blue and red semi-transparent curves. The plain curves represent the smoothed spectrums. Each black dot represent a mechanical resonance with SNR above 9. Its height corresponds to the level of the smoothed spectrum.

Finally, all mechanical resonances frequencies and SNR are summarized table 1.

At low-frequency, several mechanical resonances appear to have been detected. But many of them correspond to harmonics of lower-frequency mechanical resonances. The 2.44, 3.51, 3.81, 4.73 and 5.95 Hz are harmonics of the 1.22Hz within the 0.15Hz precision of the FFT. This mechanical resonance and its harmonics are present in the Z excitation spectrum which correspond to the long side on ESQB.

In the following, the tapping and shaking tests results of other ESQB optical components are presented. The same analysis has been applied. However, another accelerometer labelled '*Mini Acc*' was also installed on each tested optical element such that it senses acceleration noise in the direction parallel to the incident beam direction on the tested component.

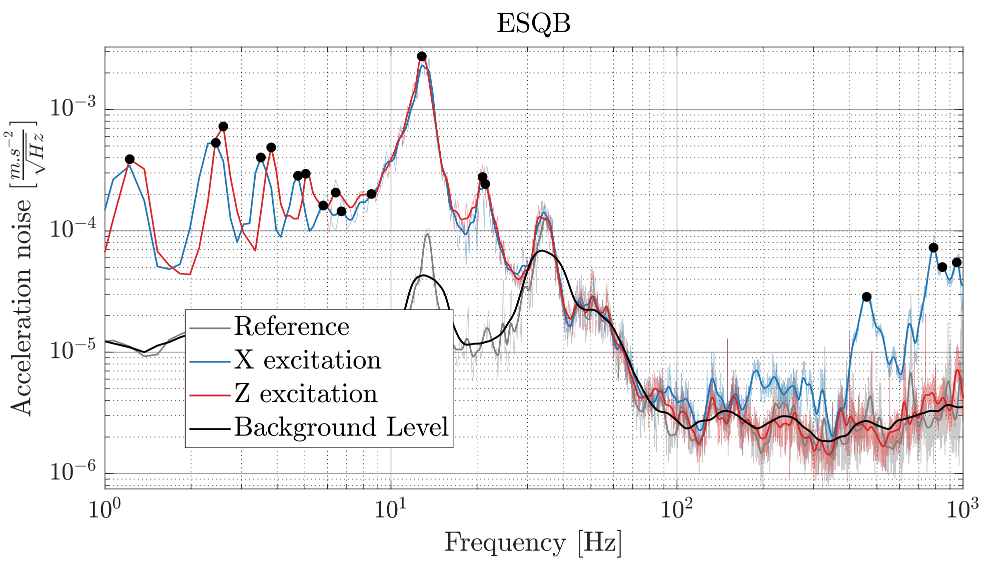

Figure 4: Shaking tests on ESQB. Each black dot represent a mechanical resonance.

- The SDB1 Viewport Pipe by which the squeezed beam is injected into the interferometer has also been tested with an X excitation which is parallel to the incident beam direction. The frequency window for the smoothing is $\frac{f}{12}$. As the SDB1 Viewport Pipe reference spectrum exhibits more peaks with respect to the floor level, the background level was estimated by using a sliding median filter with a window of $\frac{f}{2}$. This allows to extract a background level less sensitive to peaks with respect to a mean fiter.

  Here, the substraction of all 50Hz lines is also quite visible by comparing the raw and smoothed data.

  As can be seen in figure 5, only two mechanical resonances with SNR above 9 have been found.

- Both SM1 and SM2 are installed on identical mount so it can be expected that they share the same mechanical resonances. And therefore only one steering mirror has been tested. This is a critical test to do as stray-light is highly sensitive to these SMs motions.

  SM2 being the last component on ESQB, it is the most affected by SDB1 motions relative to ESQB. Indeed, the squeezed beam which follow the interferometer beam should always

Figure 5: Tapping tests on SDB1 Viewport Pipe. Each black dot represent a mechanical resonance.

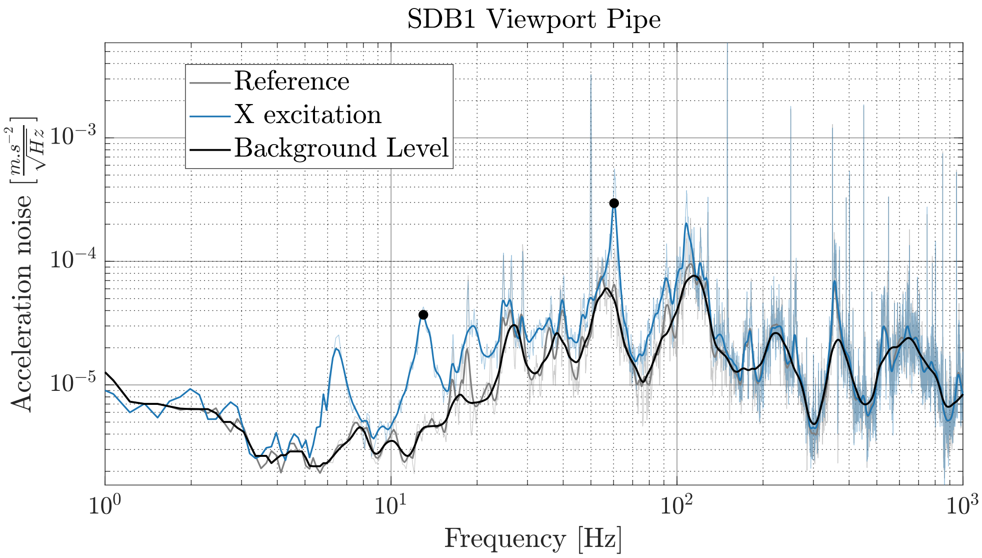

been aligned on the SM1. Furthermore both SM1 and SM2 are 1" optics installed on mount with 23 mm clear aperture with beams incident at 45° on both of them.

As can be seen figure 6, two broadband excitations are present in the excited spectrum. In order to well represent these excitations, a median filter with small windows. They are respectively $\frac{f}{32}$ and $\frac{f}{6}$ for the excited and reference spectrums. And indeed this smaller windows allow to detect peak on the shoulder of these two main excitations.

- The FIs chain should prevent scattered light from the squeezer box to be injected back into the interferometer. However FI3, which is the first Faraday Isolator that the interferometer beam will encounter, can itself be a source of back-scattered light into the interferometer. Spurious light is indeed coming from the SDB1 Faraday Isolator waveplate (as the interferometer main beam is mainly s-polarized). But the careful tuning of this waveplate can greatly decrease the amount of spurious light on the ESQB.

  ⊙ In a similar fashion to the SM analysis, a median filter with small smoothing windows has been chosen. They windows are respectively $\frac{f}{40}$ and $\frac{f}{3}$ for the excited and reference spectrums. The results are presented figure 7

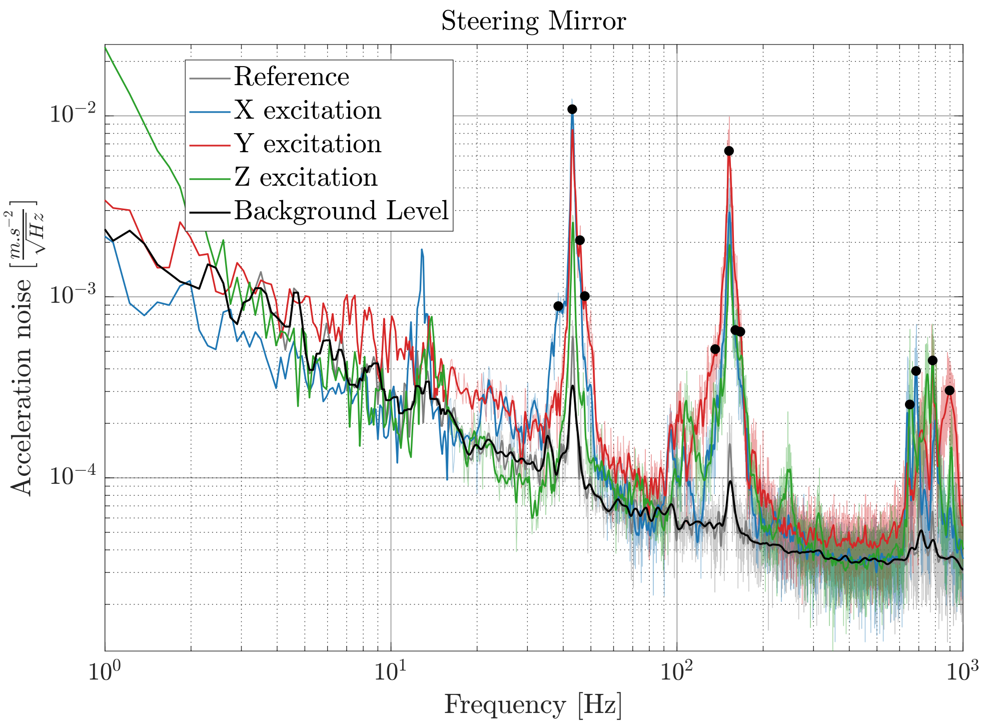

Figure 6: Tapping tests on SM mount. Each black dot represent a mechanical resonance.

- ⊙ Then the FI3 Polarizer mount base has been also tested and results are presented figure 8. Due to space constraints, only an X excitation has been performed.

  The excited spectum used a $\frac{f}{1}$ window and the background a $\frac{f}{2}$ window to apply a median filter.

- ⊙ Finally the FI3 crystal mount has been tested with results presented figure 9.

  A median filter with window of respectively $\frac{f}{26}$ and $\frac{f}{4}$ were applied for the excited and reference spectrums.

–

- The two cameras Cam Far and Cam Near can also be a source of stray-light for the interferometer as they sense the interferometer beam reflection from FI3.

  Similar to the Steering Mirrors, they are identical installed in identical mounts. Therefore, data of tapping tests performed on both cameras have been analyzed together.

  Many 50Hz are visibles in the raw signals and removed before the analysis as previously presented. A median filter with respective windows $\frac{f}{20}$ and $\frac{f}{5}$ for the excited and reference spectrums was applied.

Figure 7: Tapping tests on FI3 polarizer mount. Each black dot represent a mechanical resonance.

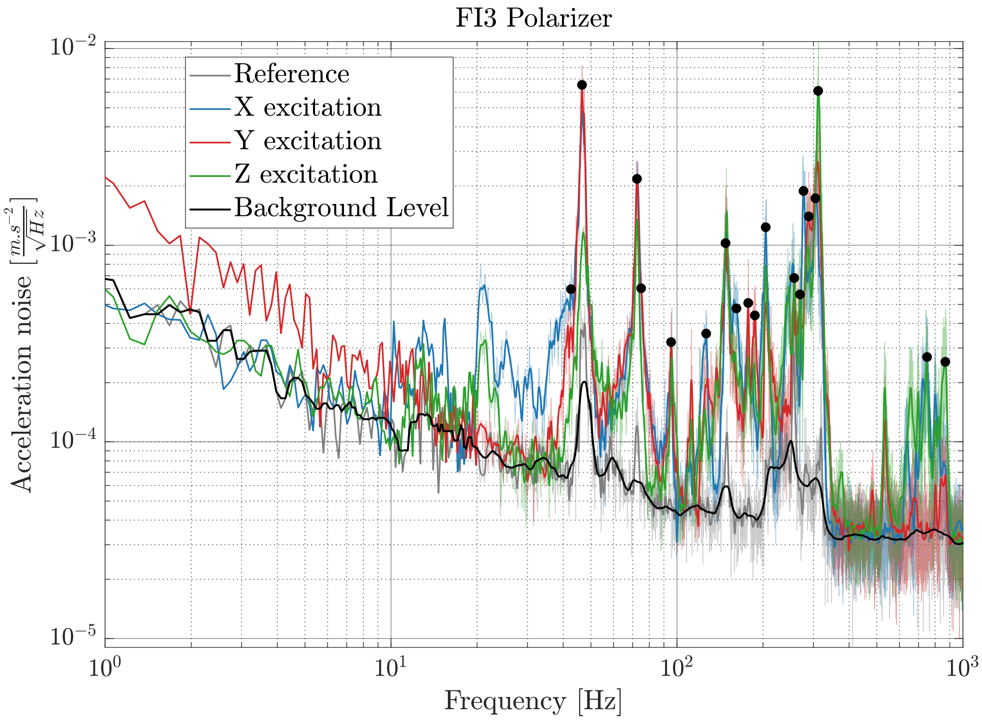

It can be seen figure 10, that 2 mechanical resonances are detected around 27Hz. They actually correspond to the same mechanical resonance but the peaks themself appear to have a small frequency shift. This brings a limit to the precision with which the mechanical resonance frequency is estimated at the order of ±0.8Hz. This precision is given by the two mechanical resonance frequencies difference. The frequency of this mechanical frequency has then been estimated as the mean of these frequencies.

All results of the tapping tests are summarized table 1.

Figure 8: Tapping tests on FI3 polarizer mount base. Each black dot represent a mechanical resonance.

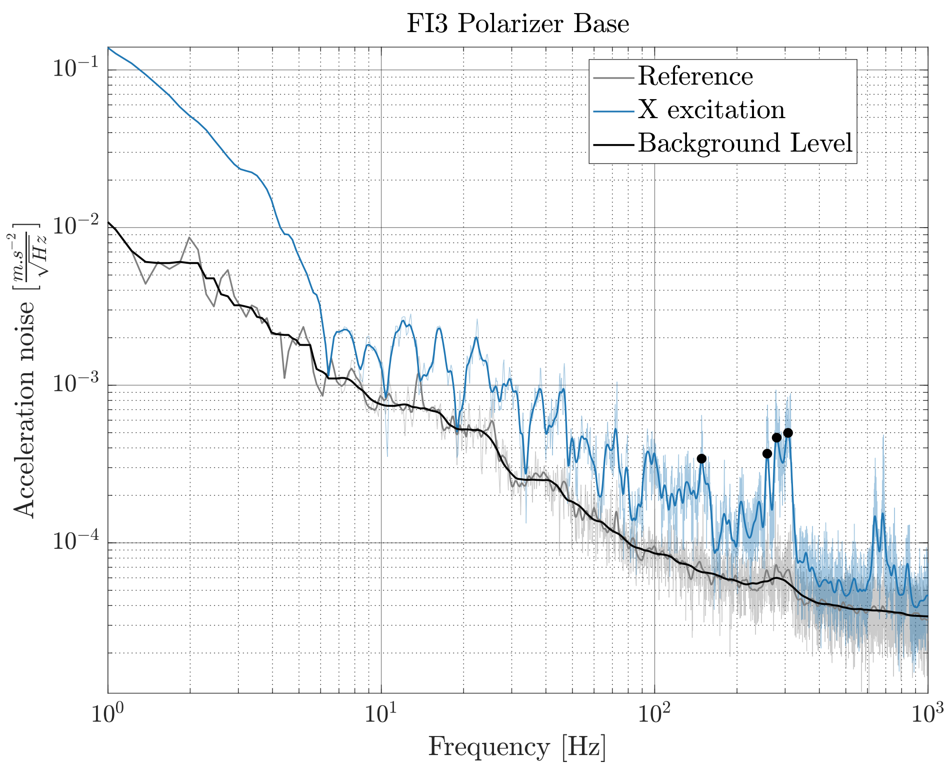

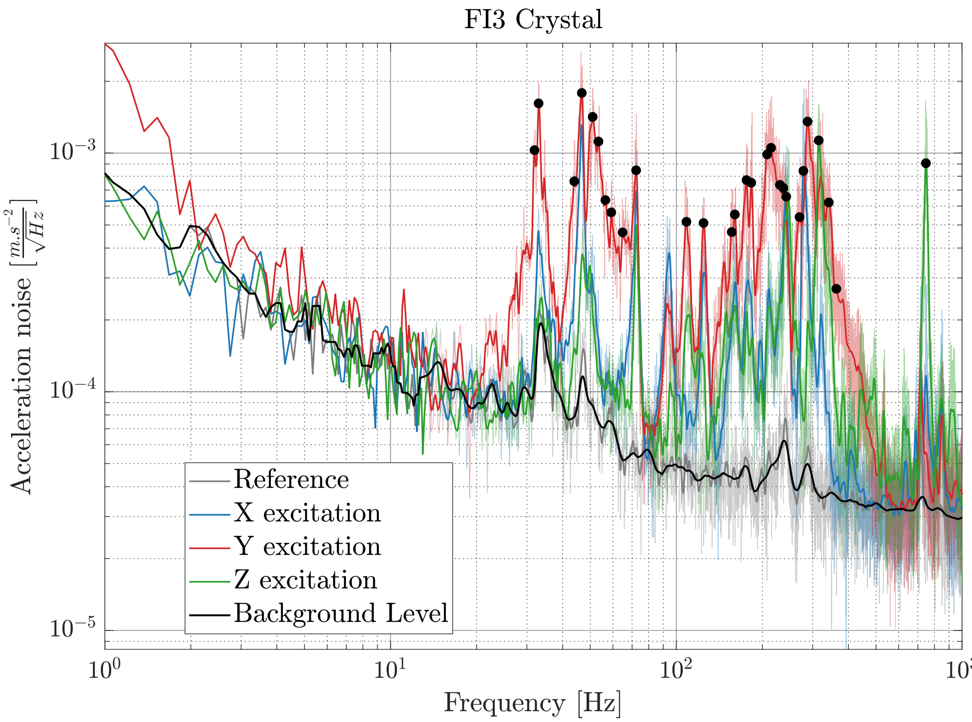

Figure 9: Tapping tests on FI3 crystal mount. Each black dot represent a mechanical resonance.

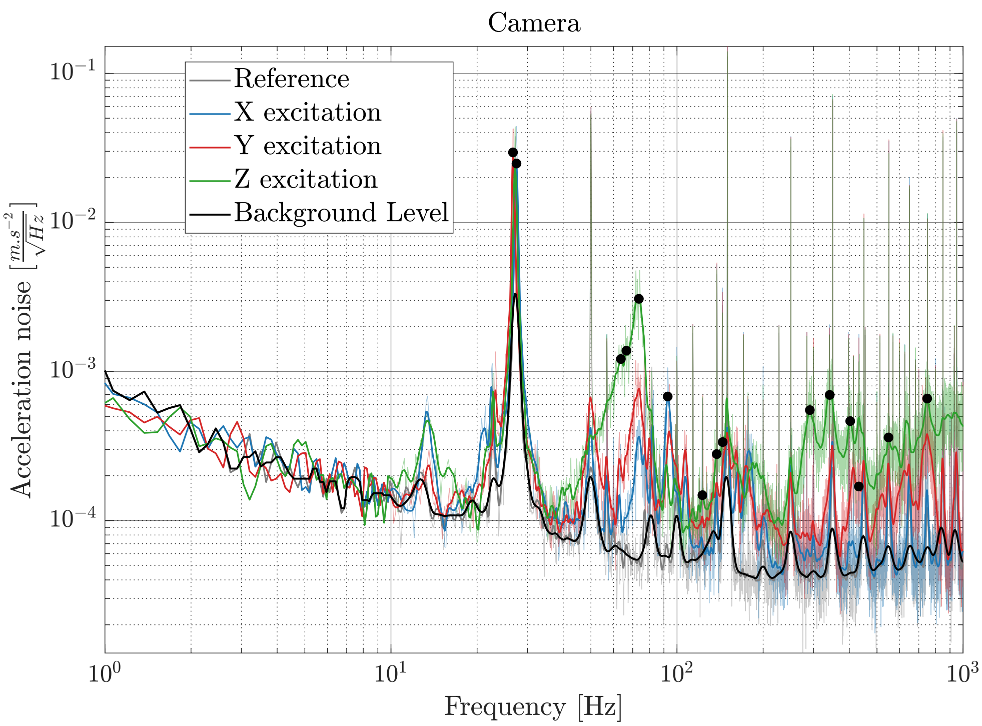

Figure 10: Tapping tests on both Cam Far and Cam Near mounts. Each black dot represent a mechanical resonance.

Frequency [Hz]	SNR	Component
Frequency [Hz]	SNR	Component
1.2	35.50	ESQB
2.4	42.79	ESQB
2.6	62.94	ESQB
3.5	55.38	ESQB
3.8	76.18	ESQB
4.7	43.66	ESQB
5.0	44.59	ESQB
5.8	25.88	ESQB
6.4	35.66	ESQB
6.7	24.16	ESQB
8.5	29.34	ESQB
12.8	76.38	ESQB
13.0	9.56	SQB1 Viewport Pipe
20.9	29.28	ESQB
21.4	19.53	ESQB
27.2	16.81	Camera
31.9	10.90	FI3 Crystal
33.0	10.90	FI3 Crystal
38.5	9.31	Steering Mirror
42.6	9.14	FI3 Polarizer
43.0	38.25	Steering Mirror
44.0	14.36	FI3 Crystal
45.8	17.38	Steering Mirror
46.5	42.06	FI3 Polarizer
46.7	16.19	FI3 Crystal
47.6	11.75	Steering Mirror
51.0	21.53	FI3 Crystal
53.4	15.70	FI3 Crystal
56.5	9.58	FI3 Crystal
59.2	10.00	FI3 Crystal
60.3	9.55	SQB1 Viewport Pipe
63.6	21.67	Camera
64.8	11.40	FI3 Crystal
66.5	28.01	Camera
72.3	23.14	FI3 Crystal
72.5	41.86	FI3 Polarizer
73.5	57.86	Camera
74.9	10.72	FI3 Polarizer
92.8	18.59	Camera
95.4	10.04	FI3 Polarizer

Continued on Next Page

Frequency [Hz]	SNR	Component
108.5	12.89	FI3 Crystal
122.7	9.08	Camera
124.5	11.07	FI3 Crystal
126.5	10.57	FI3 Polarizer
136.0	11.06	Steering Mirror
137.6	12.01	Camera
144.3	12.86	Camera
147.9	30.41	FI3 Polarizer
148.5	9.88	FI3 Polarizer Base
152.0	75.47	Steering Mirror
156.3	10.10	FI3 Crystal
159.9	10.25	Steering Mirror
160.2	11.53	FI3 Crystal
161.4	13.09	FI3 Polarizer
166.5	14.32	Steering Mirror
176.1	22.61	FI3 Crystal
177.5	16.51	FI3 Polarizer
182.9	19.70	FI3 Crystal
187.2	11.78	FI3 Polarizer
204.3	26.55	FI3 Polarizer
207.8	25.61	FI3 Crystal
214.5	19.75	FI3 Crystal
230.4	13.34	FI3 Crystal
236.8	10.82	FI3 Crystal
242.3	12.04	FI3 Crystal
257.1	13.89	FI3 Polarizer
258.0	10.38	FI3 Polarizer Base
269.3	15.11	FI3 Polarizer
269.9	16.17	FI3 Crystal
276.9	34.75	FI3 Polarizer
278.3	32.73	FI3 Crystal
279.4	11.42	FI3 Polarizer Base
287.9	32.14	FI3 Crystal
289.0	36.21	FI3 Polarizer
291.3	13.11	Camera
304.9	40.46	FI3 Polarizer
307.5	12.29	FI3 Polarizer Base
311.7	112.99	FI3 Polarizer
314.9	37.54	FI3 Crystal
341.6	21.10	FI3 Crystal
341.8	10.44	Camera

Continued on Next Page

Frequency [Hz]	SNR	Component
363.0	9.65	FI3 Crystal
403.1	12.70	Camera
432.0	29.23	Camera
460.4	10.71	ESQB
548.7	9.80	Camera
651.1	9.03	Steering Mirror
685.0	14.20	Steering Mirror
747.1	38.74	FI3 Crystal
748.9	13.26	Camera
749.4	10.81	FI3 Polarizer
782.8	12.55	Steering Mirror
788.4	25.05	ESQB
846.6	15.27	ESQB
867.9	9.08	FI3 Polarizer
897.1	9.15	Steering Mirror
950.6	15.85	ESQB

Table 1: Mechanical resonances of ESQB components with SNR above 9 with respect to a quiet reference spectrum. The frequency precision is $\pm 0.45 Hz$.

4 Mechanical resonances and Virgo sensitivity

Following these tests, the airflow has been left on inside the squeezer enclosure causing a broadband excitation of its mechanical resonances. This had a clear effect on the sensitivity as presented figure 11.

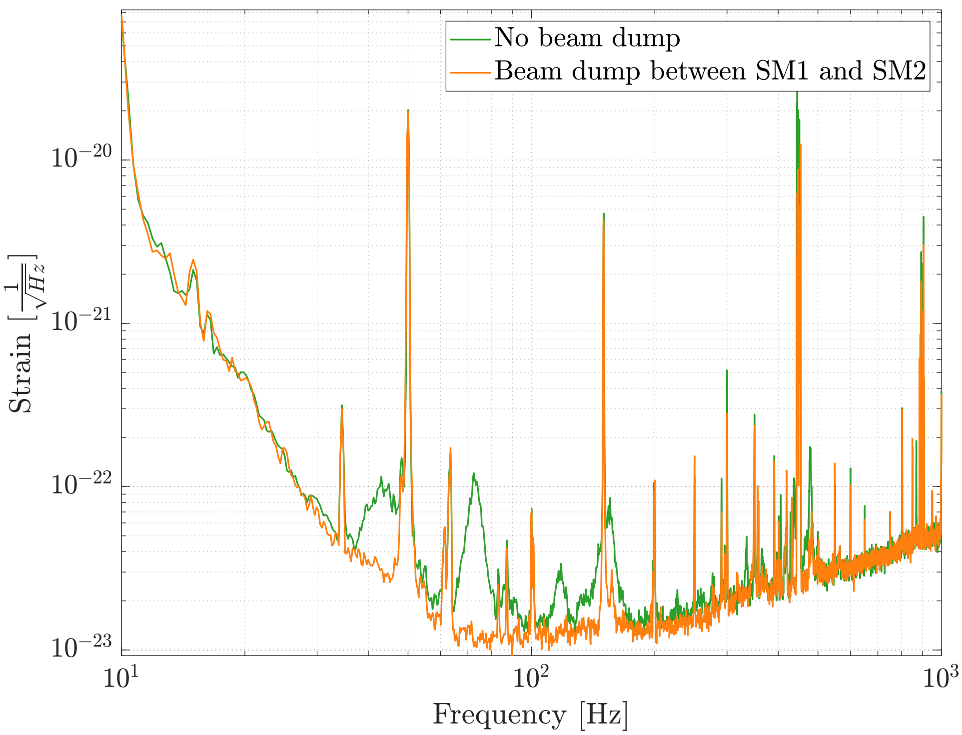

Figure 11: Effects of airflow inside the squeezer enclosure on the interferometer sensitivity with poor squeezer alignment conditions.

By comparing the excitations on this figure to the mechanical resonances of ESQB components, it can be seen that several are matching the FI3 Crystal mechanical resonances, polarizer and SM. And indeed, using an infra-red viewer, the beam was found out to be hitting the mounts of SM1 and FI3 polarizer while a spurious beam was hitting Cam Near mount. After a careful realignment, making sure that the beam was well centered on all optics and that no spurious beam was present, the degradation of the interferometer sensitivity due to back-scattered light on ESQB disappeared.

Later on, just before the O3 run, some suspect structures appeared again in the sensitivity spectrum. By comparing these structures peak frequencies to the ESQB mechanical resonances frequencies of table 1, it is possible to extract information about the incriminated components.

In this case, we could see that several mechanical resonance frequencies of the FI3 crystal and polarizer and of the camera are matching peaks on the sensitivity spectrum. By looking these components with and IR viewer, it was possible to find spurious beam on these components. Removing these beams by re-aligning the beams on the ESQB led to the removal of the peaks on the sensitivity spectrum.

Bibliography

[1] L. Conti, A. Bertolini, A. Chiummo, S. Chua, I. Fiori, E. Genin, J. Harms, M. Leonardi, G. Pillant, and J.P. Zendri. *Update on stray light noise from AEI squeezer in AdV.* (Cit. on p. 3).